Energy and AI 10 (2022) 100197

Contents lists available at ScienceDirect

Energy and AI

journal homepage: www.elsevier.com/locate/egyai

A new hybrid AI optimal management method for renewable energy communities

Francesco Conte [a], Federico D'Antoni [b], Gianluca Natrella [c], Mario Merone [b,*]

[a] Unit of Innovation, Entrepreneurship & Sustainability, Department of Engineering, Università Campus Bio-Medico di Roma, Via Alvaro del Portillo 21, Rome, 00128, Italy

[b] Unit of Computer Systems and Bioinformatics, Department of Engineering, Università Campus Bio-Medico di Roma, Via Alvaro del Portillo 21, Rome, 00128, Italy

[c] DITEN, Università degli Studi di Genova, Via all'Opera Pia 11a, Genoa, 16145, Italy

ARTICLE INFO

Keywords:
Artificial Intelligence
Deep learning
Renewable Energy Community
Battery Energy Storage System management
Model Predictive Control

ABSTRACT

In this study, we propose a hybrid AI optimal method to improve the efficiency of energy management in a smart grid such as Renewable Energy Community. This method adopts a Time Delay Neural Network to forecast the future values of the energy features in the community. Then, these forecasts are used by a stochastic Model Predictive Control to optimize the community operations with a proper control strategy of Battery Energy Storage System. The results of the predictions performed on a public dataset with a prediction horizon of 24 h return a Mean Absolute Error of 1.60 kW, 2.15 kW, and 0.30 kW for photovoltaic generation, total energy consumption, and common services, respectively. The model predictive control fed with such predictions generates maximum income compared to the competitors. The total income is increased by 18.72% compared to utilizing the same management system without exploiting predictions from a forecasting method.

1. Introduction

The 2015 Paris agreement fixed the goal of the carbon neutrality by 2050. This can be achieved by reducing the energy consumption of human activities and the greenhouse gas emissions [1]. Such a task is challenging because it requires a significant change of current power plant scenarios, including an increase in the utilization of Renewable Energy Source (RES) up to 40% of electricity supply by 2040 [2]. In this framework, the European Commission introduced in its legislation the REC, which is a legal entity representing a specific case of smart grid [3]. Its aim is to generate, store and sell renewable energy as well as exchange inside the energy produced by the units of REC itself using the public grid as distribution network. The final goal is to provide economic, environmental and social benefits of the local area where it operates [4]. REC members include residential customers, small-medium enterprises and local authorities. In the case of Italian legislation [5], a limit of 1000 kW peak for RES power plant exists, and all REC members must be connected to the same HV/MV substation. Straightforwardly, optimizing the management of a REC translates into an increase of the economic, environmental and social benefits of the community.

For the reasons above, in recent years research efforts have moved towards the development of methods to optimize the forecasting and the management of electrical energy features. Regarding REC, forecasting concerns renewable generation [6] and power demand [7]. The goal of forecasting is to predict the forthcoming values of a time series. In the case of RECs, optimal control methods usually resort to sequence-to-sequence forecasting, meaning that the predictive model receives as input a sequence of one or more features, and returns a temporal sequence of values of one or more of the features under investigation.

More in detail, a predictive model can be considered as a black-box, white-box, or gray-box [8]. In black-box models, an Artificial Intelligence (AI) model takes the features as input and directly returns the optimal action that should be performed [9]; such models often resort to Convolutional Neural Network (CNN) or Long Short-Term Memory (LSTM) neural networks for the prediction. White-box models are based on physical models that return an estimate of future values based on physical data [10]; gray-box models merge white- and black-box approaches [11].

With regards to the management of electrical energy systems, the control can be applied to Energy Storage Systems (ESSs) or to deferrable loads. In the former case, an ESS such as a rechargeable battery is managed to pursue an optimum, whether it concerns the maximization of economic function [12] or the reduction green-house gases emissions [13]. In the latter case, the cumulative load of a set of consumers is

* Corresponding author.
E-mail address: m.merone@unicampus.it (M. Merone).

https://doi.org/10.1016/j.egyai.2022.100197
Received 10 June 2022; Received in revised form 3 August 2022; Accepted 4 August 2022
Available online 6 August 2022

adapted in such a way to reduce peak load, for example by generating optimal electric vehicles charging scenarios [14].

In this framework, in our study we introduce a Time Delay Neural Network (TDNN) for the sequence-to-sequence forecasting of electrical energy features in a REC for prediction horizons length ranging from 15 min to 24 h. The TDNN achieves state-of-the-art performance in terms of forecasting error, presenting a Mean Absolute Error (MAE) that is smaller than those of the competitors we implemented and optimized on the same dataset. MAE is defined as $\sum_{t=1}^{N} |e_t|/N$ where e_t is the difference between a true and a predicted value at timestamp t, and N is the total number of timestamps considered. The predictions from each model are then passed to a newly introduced stochastic MPC algorithm in order to maximize the income of the REC by compensating the forecasting errors with a BESS. We prove that the stochastic algorithm performs better than a deterministic MPC algorithm. We refer to the proposed method as a hybrid method, in the sense that it exploits the predictions of a black-box AI model to feed a white-box mathematical management model. Utilizing the proposed hybrid method, we were able to increase the income by 18.72% compared to not performing a prediction, meaning that the current load and generation values are considered as predicted values. The income achieved corresponds to 96.73% of the maximum income achievable in the case of perfect predictions, which are the predictions that the model would provide if it had a forecasting error of 0 kW.

The main contributions of this paper are summarized as follows:

- A new hybrid AI method for efficient management of users demand and photovoltaic generation uncertainties within a REC;
- Development and optimization of a TDNN able to predict the future values of the electrical energy feature time series within a REC: common services, aggregated load, and Photovoltaic (PV) energy generation;
- Analysis of the performance of the TDNN compared with state-of-the-art electrical energy forecasting methods;
- Development of a stochastic MPC method for the optimal management of RECs including ESSs;
- Investigation of the optimal length PH of the prediction horizon to be given as input to the MPC algorithm in order to maximize the income of the REC.
- Analysis of the relation between the forecasting accuracy and the economical income of the REC.

The remainder of this paper is organized as follows: Section 1.1 provides an insight on previous works and on the motivations for the proposed method; Section 2 presents the methodology that has been followed and the main assumptions that has been made; Section 3 presents the results of the predicted electrical energy features and of the optimal control algorithms; Section 4 gathers the main conclusions of the work.

1.1. Background

REC is a legal entity introduced by the European Commission in its legislation, representing a specific case of smart grid [3]. The energy management of smart grids consists in a combination of methods and strategies to improve performance, efficiency, and energy utilization of the community [8]. In recent years, research made great efforts towards the development of green solutions, ranging from systems capable of forecasting future energy consumption and generation, to methods aiming to an optimal management of electrical energy resources in residential or industrial buildings provided with RES [8].

With regards to the forecasting of electrical energy features, studies are mainly directed towards two features to be investigated, namely energy demand and RES generation. In the case of a REC, the former refers to the amount of electrical energy that is consumed by the community members; the latter refers to the amount of green energy that is produced.

Koprinska et al. [15] proposed a CNN for the prediction of electricity load and solar PV generation from previous data of the same features gathered for two years from publicly available datasets of Australia, Spain and Portugal [16]. CNNs are used extensively as they can learn repeating features and patterns in the data automatically. The authors evaluated the performance of different architectures and parameter combinations on the validation test and selected the best one for each dataset among them. All the optimal models presents two convolutional layers with size 24 and 10, and Rectified Linear Unit (ReLU) activation function with a dropout rate of 0.5 and a 5×1 kernel size. The training was done using the stochastic gradient descent backpropagation algorithm and the Adam optimizer [17], minimizing the mean squared error. The MAEs for a prediction horizon of 24 h achieved on the solar dataset and on the three load datasets are 114.38 kW, 340.64 kW, 1884.86 kW, and 497.62 kW, corresponding to RMSEs of 153.91 kW, 476.9 kW, 2392.88 kW, and 642.52 kW, respectively.

Barzola-Monteses et al. [18] used an LSTM for the prediction of building energy consumption. LSTM neural networks are particularly suited for time-series problems where both long- and short-term dependencies between input and output data exist. The model was tested on two days of data collected from an institutional building in Ecuador. The model presents an input window of size that takes the latest 8 timestamps of normalized data and 6 hidden units with hyperbolic tangent activation function, while the output regression neuron presents linear activation. The average MAE on a 5-minute prediction horizon is 3.714 kW, corresponding to a 5.085 kW average RMSE.

Kim and Cho [19] put together the two previous approaches, proposing a combined CNN-LSTM neural network to predict the individual household electric energy consumption using two years of data presented in the University of California machine learning repository dataset [20]. The rationale of such a model lies in observing that the CNN layer is able to extract relevant spatial and temporal features from the input time series, and gives them as input to the LSTM layer which provides a prediction based on their temporal relationship. The model presents two initial convolutional layers with ReLU activation function, 64 filters and a kernel size of 2×1, each followed by a pooling layer; follows an LSTM layer with 64 units and two dense layers with 32 and 60 neurons, respectively. The last layer provides one predicted value for each minute of the coming hour (i.e., the model has a maximum prediction horizon of 60 min), achieving MAE of 0.3493 kW, corresponding to a Mean Absolute Percentage Error of 34.84% and to an RMSE of 0.6114 kW.

With regards to the methods that aim to manage RECs, two main approaches can be adopted: ESS management and/or deferrable loads management. In both cases, control can be centralized, meaning that a single controller takes decisions for the whole community, or decentralized, meaning that each member of the community can perform its own optimal control.

Olivella-Rosell et al. [21] considered a community composed of 100 houses equipped with own RES and BESS. A centralized controller operates on members' BESSs to reduce the electricity bill of each member in the case flexibility is required and in the case it is not. The authors demonstrated that the optimal centralized control results in bigger savings compared to the case of local optimal control by each member.

Barone et al. [22] introduced a REC in which the members are equipped with RES and own electric vehicles. The objective is to optimize the consumption of the energy generated by the RESs by managing the charge of the electric vehicles by means of smart metering and smart charging. The community is paid by consuming the energy generated by the RESs. The smart meters send information to a controller about members' power demand and RES generation. The controller operates on the smart chargers, charging the electric vehicles, in order to optimally exploit renewable generation.

Van Custem et al. [23] proposed a community with members having RESs, BESSs, and/or thermal energy storage systems without any aggregator. The goal of the REC is to optimize a common cost function by

reaching all members' consent. The distributed algorithm controlling the community is based on blockchain technology to ensure a safe communication between members. Each member interacts only with the blockchain and shares its flexible resources with the community. In a first step, the community plans an optimal profile of the aggregated energy demand for the following day and communicates it to the electric grid operator. Iteratively, each member optimizes its profiles given the expected optimal profiles of the other members and shares these information with the community. Each participant will adapt its profiles based on others information in order to optimize the common cost function.

Some works exist that propose a hybrid approach, i.e., that exploit an AI model to enhance the management of smart communities based on mathematical models. Wen et al. [24] presented a deep neural network with two LSTM layers to forecast residential hourly energy demand and the hourly PV energy output on aggregated power load of 40 residential buildings in Austin, Texas, from a public dataset containing one month of data [25]. The neural network takes as input a combination of schedule variables, weather variables, and timescale variable including hour of the day, day of the week, day of the month, and month of the year. The predictions of the LSTM for the aggregated demand and the PV production achieve a MAE of 2.365 kW and 4.369 kW, respectively, and they are passed as input to a Particle Swarm Optimization algorithm to optimize the load dispatch of grid-connected community microgrid, considering the uncertainties of renewable energy resources and power load simultaneously. The authors are thus able to generate scenarios for electric vehicles charging and ESS management such that load peaks are shifted, and daily costs are reduced by 8.97%.

Arkhangelski et al. [26] validated an Optimized Urban Microgrid Energy Management algorithm using one year of consumed and PV publicly available data gathered from a community in New England, USA [27]. The exploited predictive LSTM neural network achieved MAE of 16 kW and 8 kW for the one-day-ahead prediction of aggregated demand and PV generation, respectively; its predictions are given as input to the Energy Flow Management strategy to generate optimal management scenarios for the REC.

1.2. Motivations

As described in the previous section, most works only focus on the prediction of future electrical energy features, or exclusively on ESS or power demand management. In this work, we propose an end-to-end method to perform both tasks: the predictions from a neural network are given as input to a MPC algorithm to optimize a cost function.

Although white-box physical models provide interpretable outcomes extracted from physics-based equations, it has been proved that predictions from black-box models such as deep neural networks achieve equal or better results in terms of prediction errors [28]. However, the typical error measures utilized in energy forecasting tasks may not necessarily reflect the economic value of reducing forecast errors [28]. Indeed, it has been calculated that a 1% reduction in load forecasting prediction error, from a short-term unit commitment perspective, may translate into saving hundreds of thousands to millions of dollars annually [29].

For these reason, the presented hybrid AI method exploits accurate predictions of the energy features from a neural network, and provides a direct calculation of the amount of money that would be earned by utilizing the proposed optimal management method. In addition, the MAE is presented in terms of kW to provide an estimate of the quality of the AI predictor. Also, a normalized measure of the MAE with respect to the mean value of the test set is utilized, so that an estimate can be made on the economic gain if the proposed method is used on different communities. It is worth noting that the utilization of a BESS to compensate forecasting errors guarantees community income without burdens on the grid.

2. The hybrid AI optimal management method

The new hybrid AI optimal management method proposed in this study presents an end-to-end approach that takes as input the recorded energy features and outputs the maximized income that is returned by the optimal management. The method is composed of two main elements that are the AI forecasting TDNN and the stochastic MPC. More in detail, the recorded energy features are preprocessed and given as input to a TDNN for the forecasting of future values of such features. These predictions are thus passed to a stochastic MPC for the management of the BESS, and the maximized income is computed and returned. A schematic representation of the hybrid method is shown in Fig. 1. The following sections report a detailed description of the data and its preprocessing, the TDNN used for prediction, and the REC optimal management.

2.1. Data and preprocessing

The considered case-study is a publicly-available [30] aggregation of 2 years of data of fifteen consumers equipped with a common PV generation plant serving a common electrical load. The individual consumption of each consumer was added to those of all the other consumers, so that a single feature representing the aggregated energy demand was obtained. Similarly, the PV productions from single sources were summed up to generate a unique feature. The load related to the common energy demand was considered as a stand-alone feature, due to its periodicity. In addition, each electrical energy feature time series was manually coupled with 2 numerical-coded features, one representing the day of the week (ranging from 1 to 7), and one representing the timestamp of the day, following the 15-minute sampling (thus ranging from 1 to 96). In practice, we considered 3 time series of data with 3 features. Each feature was normalized separately using z-score normalization.

2.2. Time delay neural network for prediction

The energy features included in the dataset utilized in this work can be reduced to 3, namely aggregated load, total PV production, and common services. In order to perform an optimal energy management, it is fundamental to accurately predict such relevant features. Straightforwardly, we propose a Time Delay Neural Network (TDNN) for the prediction of future values of each of such features. A TDNN is efficient for modeling long-term temporal contexts, indeed, its training time is much shorter than state-of-the-art recurrent neural networks such as LSTM [31]. In particular, we resort to a sequence-to-sequence approach, i.e., the model takes as input a sequence including the past N values, and returns as a prediction a sequence of PH future values, where PH corresponds to a fixed prediction horizon, in timestamps. We consider also the day of the week and the time of the day as input. In general, after having fixed the size N of the input window, i.e. the amount of samples of the feature F to take as input at time T of a given day of the week D, the sequence of predicted values $\hat{\mathbf{F}}$ of such a feature is a vector that is a generic function of the aforementioned inputs:

$$\hat{\mathbf{F}} = f(\mathbf{F}, D, T) \tag{1}$$

In this frame, the function f varies depending on the choice of the predictive model. Regardless of the selected model, fixed a timestamp t, the input feature vector $\mathbf{F}$ is composed of a sequence of the values of such a feature $[F(t-N+1), \dots, F(t)]$, whereas the input features D and T are each represented by a single value corresponding to the time and day of the week in which the prediction is performed. In the case of the proposed TDNN, the number if input delays translates into the size of the input window, whereas no delays are considered on the hidden layer. The vector of estimated values $\hat{\mathbf{F}}$ is eventually compared to the observed values of the feature $[F(t+1), \dots, F(t+PH)]$ for performance evaluation.

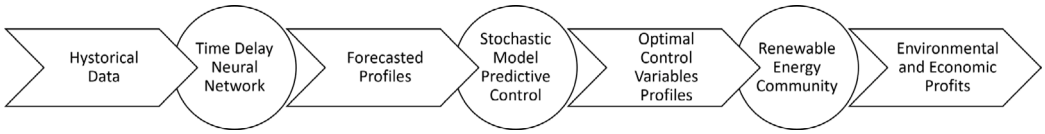

Fig. 1. Pipeline of the proposed hybrid AI method for optimal energy management.

Each feature is predicted separately, i.e., three different models are trained, each specialized in predicting only 1 out of the 3 features. The proposed TDNN is composed of an input layer receiving a data window of size N, a hidden layer with a fixed number of hidden neurons, and an output layer with 96 neurons, each corresponding to an element of the predicted sequence. In other words, considering that data have 15-minute sampling, the network produces a numeric output for each timestamp from 15 min to 24 h in the future.

During preliminary tests, we found a set of hyperparameters that provided the most promising performance for each predictive model. In detail, the learning rate is set to 10^{-2}, all neurons present hyperbolic tangent sigmoid transfer function, a regularization value of 0.3 is selected, Scaled Conjugate Gradient is set as backpropagation method [32], and the maximum number of epochs is set to 5000. Subsequently, in order to detect the optimal combination of structural hyperparameters, namely the size of the input window N and the number of hidden neurons, we performed a grid search of such parameters in the set [4, 12, 24, 48, 96, 144, 180, 200, 220, 240, 260]; these values were chosen both from preliminary tests and from works already present in the literature. The grid search was performed separately for each of energy load, production, and common services.

The dataset utilized in this work includes 2 years of monitoring. In order to obtain an unbiased estimation of the predictive performance, we first split the whole dataset into a discovery set, containing first 50% of data, and a test set, containing the remaining data. The discovery set was further split into training/validation set with 80%/20% ratio, which was shuffled at every training epoch. All features underwent z-score normalization based on the values of mean and standard deviation computed on the training set, before having been fed to the neural networks.

Each model was trained on the training set, whereas performance was evaluated on the validation set. The validation performance was constantly monitored during training for early stopping, in order to avoid overfitting. The best combination for each model according to the validation performance was finally tested for the prediction of all the 3 components, and the best performing was chosen as presented configuration. The training was thus repeated on the whole discovery set, and the performance was evaluated on the test set.

2.3. Renewable energy community optimal management

The schematic architecture of the considered REC is shown in Fig. 2. The REC is composed by a PV power plant and a BESS owned by the community and serving a group of residential buildings (the community members) and a common load. Links in Fig. 2 do not necessarily compose an actual electrical network since, according to the European directive REDII [33], the energy exchange within a REC can be virtual, with the unique condition that RESs and consumers are in the same network area. How such an area is defined is still an opened item. According to Italian transposition of the European directive IEM [34], all RECs resources and members should be connected under the same HV/MV substation. The scheme proposed in Fig. 2 is not the only one possible; however, it can represent several typical scenarios. For example, this can be the situation of a condominium with a PV generator on the roof and a common load (e.g. stairs lights), but also an area of a town where a large private prosumer (e.g. mall) or a large community prosumer (e.g. a school, the city hall, etc.) shares its RES generation with the other little consumers.

2.3.1. System model

In this subsection, the models adopted for each system component are presented. In all the following equations, t indicates the discrete-time with a sampling time Δ=15 min and the reported powers are considered as mean values within the sampling time interval.

RES. The total power generated by RES is indicated with P_t^{res}, whereas P_t^c indicates the curtailment, which must be such that

$$0 \le P_t^c \le P_t^{res} \qquad \forall t. \tag{2}$$

Connection with the main grid. During the quarter of hour t, the REC common property can export power P_t^e or import power P_t^i from the main grid. Therefore, it results that:

$$0 \le P_t^e \le P_{max}^g \delta_t^g \qquad \forall t, \tag{3}$$

$$0 \le P_t^i \le P_{max}^g \left(1 - \delta_t^g\right) \qquad \forall t, \tag{4}$$

$$P_t^g = P_t^e - P_t^i \qquad \forall t, \tag{5}$$

where: P_t^g is the power that the REC exchange with the grid; P_{max}^g is the maximum power that the REC can exchange with the grid and δ_t^g is a binary variable, that determines if the REC common property is importing ($\delta_t^g = 1$) or exporting ($\delta_t^g = 0$) power.

BESS. The BESS is able to absorb power increasing its SoC and to generate power decreasing its SoC. The evolution of the SoC over time is described by the following equation:

$$SoC_{t+1} = SoC_t + \frac{\Delta}{E}\left(\eta^{ch} P_t^{ch} + \frac{1}{\eta^{dsc}} P_t^{dsc}\right) \qquad \forall t, \tag{6}$$

$$SoC^{min} \le SoC_t \le SoC^{max} \qquad \forall t, \tag{7}$$

where: SoC_t is the current SoC of the BESS; η^{ch} and η^{dsc} are the efficiencies of the BESS when increasing and decreasing its SoC, respectively; E is the BESS capacity. The following constraints set the functioning of the BESS:

$$0 \le P_t^{ch} \le P_{max}^{ch} \delta_t^b \qquad \forall t, \tag{8}$$

$$P_{min}^{dsc}\left(1 - \delta_t^b\right) \le P_t^{dsc} \le 0 \qquad \forall t, \tag{9}$$

where: $P_{max}^{ch} \ge 0$ is the maximum power that the BESS can absorb; $P_{min}^{dsc} \le 0$ is the maximum power, in absolute value, that the BESS can generate and δ_t^{ch} and δ_t^{dsc} are binary variables. Finally, in order to limit the number of cycles of charge and discharge, the following constraints can be set:

$$\frac{\Delta \eta^{ch}}{E} \sum_{k=0}^{PH-1} P_{t+k}^{ch} \le \alpha \qquad \forall t, \tag{10}$$

$$-\frac{\Delta}{\eta^{dsc} E} \sum_{k=0}^{PH-1} P_{t+k}^{dsc} \le \alpha \qquad \forall t, \tag{11}$$

where α is a constant parameter whose value corresponds to the maximum number of charge and discharge cycles that can be done over the Prediction Horizon (PH).

REC. According to Italian transposition of the European directives IEM [34] and RED II [33], a REC is paid for the renewable energy sold to the market, as usual, and for the renewable energy shared within the community. Referring to the scheme in Fig. 2, the "shared" energy is defined as the portion of the exported renewable energy $\Delta \cdot P_t^e$, consumed by the REC members within the same time interval. More

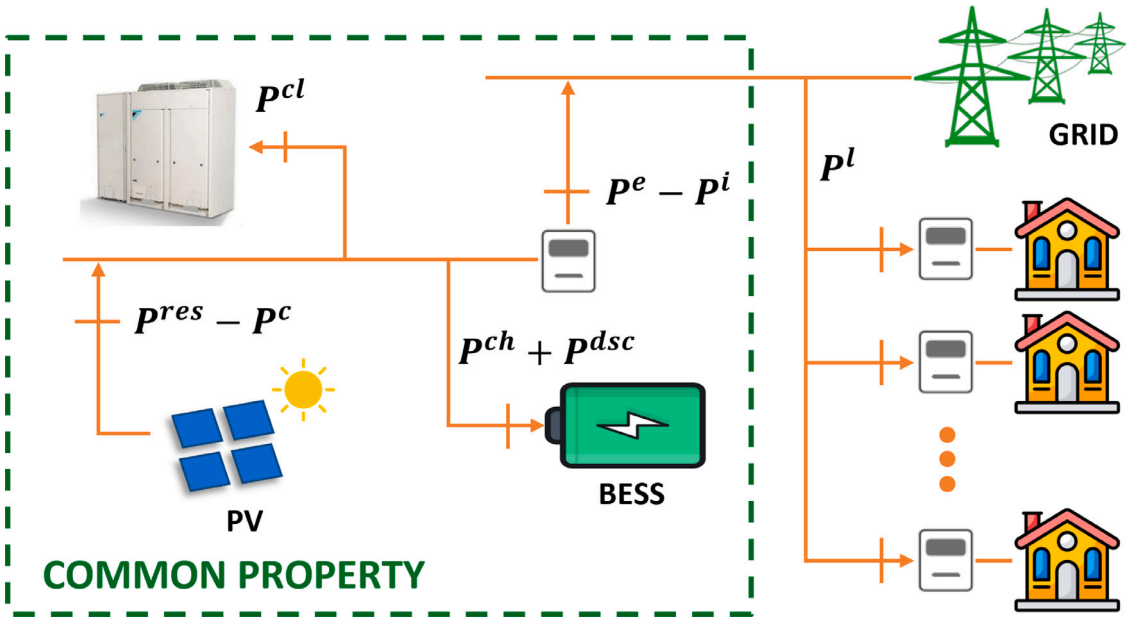

Fig. 2. REC architecture.

formally, the shared energy $\Delta \cdot P_t^{sh}$ in the quarter of hour t is defined as the minimum between the energy exported by the manager and the energy consumed by the members of the REC. Therefore, it has to result:

$$P_t^{sh} = \min\left(P_t^e, P_t^l\right) \qquad \forall t, \tag{12}$$

where P_t^{sh} and P_t^l are the shared power and the expected aggregated power demand of the residential buildings at timestamp t, respectively. According to the REC economical return (18), introduced below, both P_t^{sh} and P_t^e will be maximized and (12) can be rewritten with the following inequalities:

$$P_t^{sh} \geq 0 \qquad \forall t, \tag{13}$$

$$P_t^{sh} \leq P_t^e \qquad \forall t, \tag{14}$$

$$P_t^{sh} \leq P_t^l \qquad \forall t. \tag{15}$$

Finally, in a REC the power to charge the BESS has to be green, therefore it has to be:

$$P_t^{ch} \leq P_t^{res} - P_t^c \qquad \forall t, \tag{16}$$

where P_t^{res} is the expected power generated by the RES in the quarter of hour t.

Power balance, operational costs and available data. During the operations, the following power balance has to be matched:

$$P_t^{res} + P_t^i = P_t^{ch} + P_t^{dsc} + P_t^e + P_t^c + P_t^{cl} \qquad \forall t, \tag{17}$$

where: P_t^{cl} is the expected common power demand during the quarter of hour t. The REC economic return is:

$$J_t = \Delta\left((c^m + c^r)\, P_t^{sh} + c_t^e \left(P_t^e - P_t^i\right) - c^c\, P_t^c\right) \qquad \forall t, \tag{18}$$

where: c_t^e is the energy sell-back price; c^c is a penalty on the curtailed green energy; c^m is an incentive bestowed by the Italian Ministry of Economic Development (MISE) and c^r is the restitution of grid charges since the shared consumed power does not burden on the grid [5]. The objective of the paper is to maximize the REC economical return, assuming that at timestamp t, given the prediction horizon of length PH, the following data are available:

- a predicted profile of RES generation $\{P_{t+k}^{res}\}_{k=0}^{PH-1}$ with an associated vector of forecasting error variance $\{\psi_{t+k}^{res}\}_{k=0}^{PH-1}$;
- two predicted profiles of power demands $\{P_{t+k}^{cl}\}_{k=0}^{PH-1}$ and $\{P_{t+k}^{l}\}_{k=0}^{PH-1}$, both with their vectors of forecasting error variance $\{\psi_{t+k}^{cl}\}_{k=0}^{PH-1}$ and $\{\psi_{t+k}^{l}\}_{k=0}^{PH-1}$;
- the current SoC, SoC_t;
- all energy prices from timestamp t to timestamp $t + PH - 1$.

2.3.2. Optimal management algorithms

In this section, we introduce two algorithms for the optimal management of the REC. Both control algorithms perform the REC management according to the available information listed above. The decision process at any timestamp t is shown in Fig. 3: the Neural Network collects the last measurements from the REC components and computes the updated forecasts; using these forecasts, together with the current BESS SoC and the energy prices, the MPC controller determines the BESS power exchange set-points, P_t^{ch} and P_t^i.

The first algorithm is a deterministic MPC in which the forecast errors are not taken into account during optimization. In this case, during operation, forecast errors are compensated by varying the power exchange with the main grid. The second algorithm is a stochastic MPC that takes into account the probability of incurring in forecasting errors during optimization. In this other case, during operation forecast errors are compensated by modifying the BESS power exchange.

At the quarter of hour t, we will indicate with $k = 0, 1, \ldots, PH - 1$ the time sequence $t, t+1, \ldots, t+PH-1$.

Deterministic algorithm. The optimal management algorithm is based on the technique of MPC. This control method applies the so-called *receding horizon principle*, that consists, for our specific case, in the following steps to be repeated at any considered timestamp t (recalling that $k = 0, 1, \ldots, PH-1$ indicates the time sequence $t, t+1, \ldots, t+PH-1$):

- solve the following Mixed Integer Linear Problem (MILP)

$$\max_{\{U_k\}} \sum_{k=0}^{PH-1} J_k$$
$$U_k = \left[P_k^i, P_k^e, P_k^{ch}, P_k^{dsc}, P_k^c, \delta_k^g, \delta_k^b\right]^\top \tag{19}$$

  subject to (2)–(11) and (13)–(17), over a finite PH $(0, 1, \ldots, PH-1)$, obtaining an optimal control trajectory $\{U_k^*\}_{k=t}^{t+PH-1}$ as a result;
- apply only the first element of the optimal control trajectory $\{U_k^*\}_{k=t}^{t+PH-1}$.

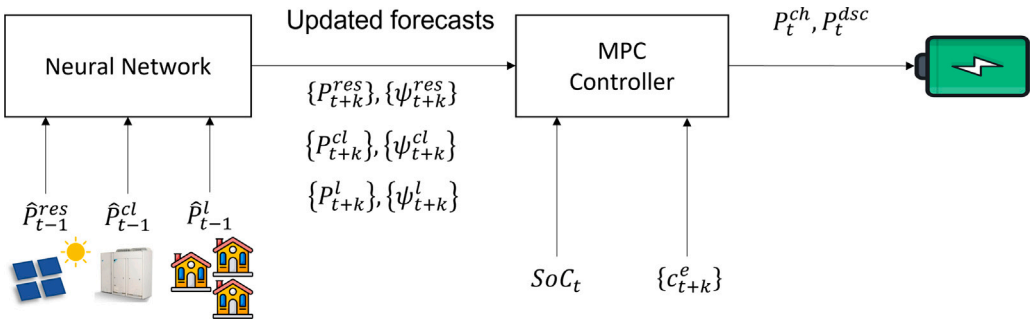

Fig. 3. Decision framework.

In this way, the control decision is computed at any considered timestamp t according to updated measurements of the system state and to updated forecasts. This guarantees a quite robust control with respect to modeling and forecasting errors. In fact, the receding horizon principle allows to make MPC a closed-loop control method, since controls are computed based on the feedback coming from the system measurements. Furthermore, by applying only the first element of the optimal control trajectory $\{U_k^*\}_{k=t}^{t+PH-1}$ it is possible, at any timestamp t and before performing the optimal control, to correct the forecasting errors that have been made at the previous timestamp $t-1$. This is done by changing the values of the power exchanged by the REC with the main grid.

Let us indicate with $\hat{P}_t^{res}$, $\hat{P}_t^{cl}$ and $\hat{P}_t^{l}$ the real value of the power generated by the RES, the real common power demand and the real aggregated power demand respectively. Since the power balance in (17) has to be always satisfied, it results:

$$\hat{P}_t^{i} = \max\left(0, P_t^{ch} + P_t^{dsc} + P_t^{c} + \hat{P}_t^{cl} - \hat{P}_t^{res}\right) \qquad \forall t, \tag{20}$$

$$\hat{P}_t^{e} = \max\left(0, -P_t^{ch} - P_t^{dsc} - P_t^{c} - \hat{P}_t^{cl} + \hat{P}_t^{res}\right) \qquad \forall t, \tag{21}$$

where $\hat{P}_t^{i}$ and $\hat{P}_t^{e}$ are the actual powers that the REC imports and exports, respectively. Therefore the actual shared power between the community members $\hat{P}_t^{sh}$ at time t is:

$$\hat{P}_t^{sh} = \min\left(\hat{P}_t^{e}, \hat{P}_t^{l}\right) \qquad \forall t, \tag{22}$$

and the REC actual income at time t is:

$$\hat{J}_t = \Delta\left((c^m + c^r)\,\hat{P}_t^{sh} + c_t^{e}\left(\hat{P}_t^{e} - \hat{P}_t^{i}\right) - c^c\,P_t^{c}\right) \qquad \forall t. \tag{23}$$

Stochastic algorithm. In this section, we propose the stochastic MPC algorithm to perform the optimal management of the operations at each timestamp t, given the available information.

To cope with the uncertainties in RES generation and power demands forecasts, the manager of the REC can control the BESS to guarantee a sufficient energy reserve. In order to evaluate the potential energy reserve that can be provided by the BESS during the quarter of hour t, the maximal positive and negative variations of the charging and discharging power are introduced, namely $\overline{\Delta P}_k^{ch} \geq 0$, $\overline{\Delta P}_k^{dsc} \geq 0$, $\underline{\Delta P}_k^{ch} \leq 0$ and $\underline{\Delta P}_k^{dsc} \leq 0$. When applied, these variations will result in two deviations of the BESS power profile, $P_k^b = P_k^{ch} + P_k^{dsc}$, a positive one and a negative one:

$$\overline{\Delta P}_k^{b} = \overline{\Delta P}_k^{ch} + \overline{\Delta P}_k^{dsc} \qquad \forall k \in [0, PH-1], \tag{24}$$

$$\underline{\Delta P}_k^{b} = \underline{\Delta P}_k^{ch} + \underline{\Delta P}_k^{dsc} \qquad \forall k \in [0, PH-1], \tag{25}$$

which can be used to stem the consequences of forecasting errors. Given the maximal variations of BESS power profile, the maximal positive and negative deviations from the SoC profile, namely $\overline{SoC}_k$ and $\underline{SoC}_k$, are $\forall k \in [0, PH-1]$:

$$\overline{SoC}_k = \overline{SoC}_{k-1} + \frac{\Delta}{E}\left(\eta^{ch}\left(P_k^{ch} + \overline{\Delta P}_k^{ch}\right) + \eta^{dsc}\left(P_k^{dsc} + \overline{\Delta P}_k^{dsc}\right)\right), \tag{26}$$

$$\underline{SoC}_k = \underline{SoC}_{k-1} + \frac{\Delta}{E}\left(\eta^{ch}\left(P_k^{ch} + \underline{\Delta P}_k^{ch}\right) + \eta^{dsc}\left(P_k^{dsc} + \underline{\Delta P}_k^{dsc}\right)\right). \tag{27}$$

The profiles in (26) and (27) are completed by the following constraints and initial conditions:

$$0 \leq P_k^{ch} + \overline{\Delta P}_k^{ch} \leq P_{max}^{ch}\,\overline{\delta}_k^{b} \qquad \forall k \in [0, PH-1] \tag{28}$$

$$0 \leq P_k^{ch} + \underline{\Delta P}_k^{ch} \leq P_{max}^{ch}\,\underline{\delta}_k^{b} \qquad \forall k \in [0, PH-1] \tag{29}$$

$$P_{max}^{dsc}\left(1 - \overline{\delta}_k^{b}\right) \leq P_k^{dsc} + \overline{\Delta P}_k^{dsc} \leq 0 \qquad \forall k \in [0, PH-1] \tag{30}$$

$$P_{max}^{dsc}\left(1 - \overline{\delta}_k^{b}\right) \leq P_k^{dsc} + \underline{\Delta P}_k^{dsc} \leq 0 \qquad \forall k \in [0, PH-1] \tag{31}$$

$$\underline{\delta}_k^{ch} + \underline{\delta}_k^{dsc} \leq 1 \qquad \forall k \in [0, PH-1] \tag{32}$$

$$\overline{SoC}_k \leq SoC^{max} \qquad \forall k \in [0, PH-1] \tag{33}$$

$$\underline{SoC}_k \geq SoC^{min} \qquad \forall k \in [0, PH-1] \tag{34}$$

$$\overline{\Delta P}_k^{ch} + \overline{\Delta P}_k^{dsc} \geq \sigma_k^{b}\theta_k \qquad \forall k \in [0, PH-1] \tag{35}$$

$$\underline{\Delta P}_k^{ch} + \underline{\Delta P}_k^{dsc} \leq -\sigma_k^{b}\theta_k \qquad \forall k \in [0, PH-1] \tag{36}$$

$$\overline{SoC}_0 = SoC_{t-1} \tag{37}$$

$$\underline{SoC}_0 = SoC_{t-1} \tag{38}$$

where $\overline{\delta}_k^{b}$ and $\underline{\delta}_k^{b}$ are binary variables that identifies the charge and discharge activation states for the two SoC trajectories. θ_k and σ_k^{b} are defined as it follows:

$$\theta_k = \sqrt{2}\,\mathrm{erf}^{-1}(1 - 2\beta_k) \qquad \sigma_k^{b} = \sum_{j=0}^{k}\left(\sqrt{\psi_j^{res} + \psi_j^{cl} + \psi_j^{l}}\right).$$

where β_k is the reliability involving the chance constraints. The number of charge and discharge cycles are limited as it follows:

$$\frac{\Delta\eta^{ch}}{E}\sum_{k=0}^{PH-1}\left(P_k^{ch} + \overline{\Delta P}_k^{ch}\right) \leq \alpha \qquad \forall k \in [0, PH-1], \tag{39}$$

$$-\frac{\Delta}{\eta^{dsc}E}\sum_{k=0}^{PH-1}\left(P_k^{dsc} + \underline{\Delta P}_k^{dsc}\right) \leq \alpha \qquad \forall k \in [0, PH-1]. \tag{40}$$

The problem to be solved at each timestamp t is the following:

$$\max_{\{U_k\}} \sum_{k=0}^{PH-1} J_k$$
$$U_k = \left[P_k^{i}, P_k^{e}, P_k^{ch}, P_k^{dsc}, P_k^{c}, \overline{\Delta P}_k^{ch}, \underline{\Delta P}_k^{ch}, \overline{\Delta P}_k^{dsc}, \underline{\Delta P}_k^{dsc}, \delta_k^{g}, \delta_k^{b}, \overline{\delta}_k^{b}, \underline{\delta}_k^{b}\right]^{\top} \tag{41}$$

subject to (2)–(4), (8), (9), (13)–(17), (24)–(40), over a finite PH $(0, 1, \ldots, PH-1)$, obtaining an optimal control trajectory $\{U_k^*\}_{k=t}^{t+PH-1}$ as a result. Only the first element of the optimal control trajectory $\{U_k^*\}_{k=t}^{t+PH-1}$ is applied and forecasts errors are corrected by changing the output powers of the BESS, exploiting the reserve energies that the algorithm has granted. Therefore, by (17) it has to be:

$$\hat{P}_t^{ch} = \max\left(0, P_t^{i} - P_t^{e} - P_t^{c} - \hat{P}_t^{cl} + \hat{P}_t^{res}\right) \qquad \forall t, \tag{42}$$

$$\hat{P}_t^{dsc} = \min\left(0, P_t^{i} - P_t^{e} - P_t^{c} - \hat{P}_t^{cl} + \hat{P}_t^{res}\right) \qquad \forall t, \tag{43}$$

Table 1
Results of the optimal configurations of the proposed model, based on different size of the input window (Input dim.) and number of hidden neurons (Nr. hidden). The results on the test set are reported in terms of MAE [kW] for prediction horizons of 15 min, 1, 12, 18 and 24 h, together with the average MAE over all the prediction horizons, and the corresponding average NMAE.

Input dim.	Nr. hidden	15 min	1 h	12 h	18 h	24 h	Mean MAE	Mean NMAE
PV generation								
4	96	1.650	2.450	5.450	5.200	3.350	4.700	0.612
180	200	1.550	2.000	3.600	2.950	3.600	2.850	0.376
200	200	1.600	2.000	2.950	3.600	2.950	2.850	0.369
240	260	1.550	1.450	1.400	1.500	1.600	1.500	0.066
Aggregated demand								
4	96	1.743	2.039	2.113	2.113	2.150	2.113	0.178
180	200	1.743	2.076	2.113	2.150	2.187	2.150	0.181
200	200	1.743	2.039	2.113	2.187	2.150	2.150	0.180
240	260	1.743	2.039	2.113	2.113	2.150	2.113	0.178
Common Services								
4	96	0.240	0.480	0.530	0.490	0.430	0.540	0.119
180	200	0.260	0.270	0.290	0.300	0.290	0.290	0.065
200	200	0.270	0.280	0.280	0.280	0.300	0.290	0.063
240	260	0.310	0.290	0.290	0.300	0.320	0.300	0.065

where $\hat{P}_t^{ch}$ and $\hat{P}_t^{dsc}$ are the actual charge and discharge powers of the BESS, respectively. The actual expression of SoC will be:

$$SoC_{t+1} = SoC_t + \frac{\Delta}{E}\left(\eta^{ch}\hat{P}_t^{ch} + \frac{1}{\eta^{dsc}}\hat{P}_t^{dsc}\right) \qquad \forall t. \tag{44}$$

3. Results and discussion

In this section, we present the results of the optimization of the proposed TDNN model and of the competitors, together with the prediction errors they achieve for different prediction horizons. Then, we present and discuss how these results translate into income due to the stochastic MPC.

3.1. Results of the predictive AI model

A grid search was performed to determine the optimal TDNN model structural hyperparameters. During the training phase, the models were trained to minimize the MAE. Nonetheless, since in this work we are addressing a sequence-to-sequence regression problem, it is not straightforward to determine what evaluation metric should be taken into account to compare models between each other, because a performance can be computed for each prediction horizon during the evaluation phase on the validation set. Consequently, we chose to take into account the configurations that resulted in the best performance for the shortest (15 min), a short-term (1 h), two intermediate (12 and 18 h), the longest (24 h), and the average of all the 96 considered prediction horizons. In this way, a subset of possible best configurations was identified for each of PV production, aggregated demand, and common services. It is worth noting that some configurations resulted to perform best for different sets of data or prediction horizons. Finally, all the possible best configurations were trained from scratch on each set of data, and tested on community for energy management.

Table 1 reports the results on the test set of the best combinations of parameters resulted from the grid searches for each of energy production, demand, and common services. The results are reported for different prediction horizons, and the average MAE for all the prediction horizons is shown for any of the sets of data considered. In addition, we reported the average Normalized MAE (NMAE) over all the prediction horizons for each configuration, defined as $NMAE = MAE/\bar{x}$, where $\bar{x}$ is the mean value of the ground-truth sequence with respect to which the MAE is normalized, i.e. the evaluation set. This latter metric provides an immediate insight on the magnitude of the prediction error, as it is scaled to the magnitude of the data under consideration, and thus allows to compare the prediction results of different features although they have different magnitude, and to compare the proposed model to others in the literature that performed tests on different datasets from ours. The predictions generated from each of the configurations presented in Table 1 were finally given as input to REC. It is worth noting how the best performance is achieved for the common services, with regards to both the absolute error and its normalized version. This may be due to the regularity and periodicity of such a feature, which presents small variations in the short term, and between one day and the following. The TDNN configurations including a larger number of hidden neurons and wider input windows perform better; the predictions from different configurations are statistically different (taken any couple of prediction sequences, paired T-test p-value $\leq 10^{-4}$). With regards to the aggregated energy demand, taking into account the NMAE, it results to be the most difficult feature to predict accurately; this may be due to sudden variation in the single demand that make the pattern less regular. No TDNN configuration performs clearly better than the others on this specific task; indeed, according to a paired T-test, these predictions are not statistically different. With regards to the PV generation, the prediction strongly benefits from a larger size of the input window (240 timestamps) and a bigger number (200) of hidden neurons. The predictions from different configurations are statistically different (taken any couple of prediction sequences, paired T-test p-value $\leq 10^{-4}$). Although this behavior is not clearly observed for other features, the combination of an input window of 240 timestamps and 200 hidden neurons always provides results that are close to the best result for each feature.

3.1.1. Results of the predictions of the competitors

In order to compare the performance of the proposed model to other state-of-the-art neural networks for time series and for energy load forecasting, we implemented and optimized several other competitors. For each of them, we used the same fixed hyperparameters and repeated the same grid search procedure performed for the proposed TDNN, including the normalization step. We utilized for all the competitors the same training/validation/test set split considered for the proposed model. To avoid overfitting, a regularization value of 0.3 was used along with early stopping techniques based on the validation set performance. Where possible, we investigated the same range of structural hyperparameters. The optimal set of parameters was identified for each model; these combinations were tested on the test set and their predictions were given as input to REC. The investigated competitors and their optimal configurations are s follows:

- An LSTM recurrent neural network with 1 hidden layer (LSTM1). The size of the input window and the number of nodes were the same tested for the TDNN. One configuration resulted the best for any test. It has an input window of size 96 (i.e. the latest 24 h of data) while the optimal number of hidden units is 180.

Table 2
Results of the optimal configurations of the competitors. The results on the test set are reported in terms of MAE [kW] for prediction horizons of 15 min, 1, 12, 18 and 24 h, together with the average MAE of all the prediction horizons, and the respective average NMAE.

Model and configuration	15 min	1 h	12 h	18 h	24 h	Mean MAE	Mean NMAE
PV generation							
LSTM1 (96-180)	4.650	4.650	4.650	4.650	4.650	4.650	0.604
LSTM2 (96-200)	4.800	4.800	4.750	4.800	4.800	4.800	0.612
biLSTM (96-200)	4.800	4.750	4.800	4.750	4.800	4.750	0.618
CNN–LSTM (96-2 × 1-32-48)	6.300	6.200	6.300	6.250	6.250	6.350	0.921
CNN–LSTM (96-2 × 1-64-64)	5.645	6.060	6.450	8.745	5.815	7.115	0.927
Aggregated demand							
LSTM1 (96-180)	2.410	2.410	2.410	2.410	2.410	2.410	0.204
LSTM2 (96-200)	2.336	2.336	2.299	2.299	2.336	2.336	0.196
biLSTM (96-200)	2.410	2.410	2.410	2.410	2.410	2.410	0.203
CNN–LSTM (96-2 × 1-32-48)	3.077	3.077	3.077	3.077	3.077	3.151	1.020
CNN–LSTM (96-2 × 1-64-64)	3.559	3.726	3.659	3.548	3.467	3.926	0.331
Common Services							
LSTM1 (96-180)	0.510	0.560	0.580	0.620	0.570	0.550	0.121
LSTM2 (96-200)	0.440	0.450	0.450	0.440	0.440	0.450	0.098
biLSTM (96-200)	0.450	0.450	0.440	0.450	0.440	0.450	0.098
CNN–LSTM (96-2 × 1-32-48)	1.300	4.530	4.530	1.580	1.300	1.610	0.357
CNN–LSTM (96-2 × 1-64-64)	1.342	1.145	1.465	1.537	1.411	1.649	0.364

- An LSTM with 2 hidden layers (LSTM2). The first hidden layer presents double the number of nodes of the second layer; the range of values investigated for the input window and the number of nodes in the second hidden layer are the same of the TDNN. This model was presented in [35]. The configuration with an input window of 96 timestamps resulted the best for any test, having 200 hidden units.
- An LSTM with one hidden layer and bidirectional connections (biLSTM). The size of the input window and the number of nodes are the same tested with the TDNN. An input window of 96 timestamps resulted the best in any test. The best choices for the hidden units is 200.
- A CNN–LSTM neural network with two 2D-convolutional layers followed by one LSTM layer and a dense layer with 32 neurons. The size of the input window and the number of LSTM nodes are the same tested for the TDNN; the number of convolutional filters tested for both the convolutional layers is in the range [2, 5, 10, 32, 64, 128]. The configuration that performed best in any test has an input window size of 96 and size 2×1 for 32 convolutional filters, followed by 48 LSTM cells. This model was presented in [19], and achieves state-of-the-art performance for a PH of one hour; straightforwardly, we also implemented the configuration they proposed, which is composed of 64 convolutional filters and 64 LSTM units.

The results achieved by all the considered configurations of the competitors are reported in Table 2. Taking into account the NMAE, it can be observed that, similarly to the TDNN, the best performance is achieved for the prediction of the common services, followed by the aggregated demand, whereas the PV generation results in larger errors. It is worth noting that the LSTM2 with the 96–200 configuration achieves, on average, the best prediction results between the competitors; nonetheless, all the competitors produce predictions that are worse than those of the proposed TDNN. In particular, the best predictions for PV generation are considerably worse than those produced by the TDNN (MAE of 4.65 kW vs 1.5 kW). Interestingly, the LSTM1, LSTM2, and biLSTM models always achieve better performance than the CNN–LSTM models. This may be due to the long prediction horizons taken into account in this study, while the CNN–LSTM model proved to be particularly effective when considering PHs of 60 min or less [19].

3.2. Optimal management results

The considered case-study is an aggregation of fifteen consumers equipped with a common PV generation plant serving a common electrical load. This system was supposed to be established as a REC located in Italy undergoing Italian regulation [5]. The general parameters of the REC are reported in Table 3. Data of common power demand P^{cl}, aggregated power demand P^{l} and PV generation P^{res} were taken from [30]. In particular, the effective reported power demand profiles of P^{cl} and P^{l} were considered, while the PV generation was increased in nominal power with respect to reference values.

All the forecasting methods were tested on both the algorithms presented in Section 2.3.2. Furthermore, the above mentioned forecasting methods were compared with the cases in which the predictions used in the optimal algorithms were 100% correct, called "ORACLE" method, and in which the predictions used were fake, called "NO-PRED" method. In particular, in the latter the predictions used for the PV generation, the common power demand and the aggregated power demand at time t are constant vectors of the corresponding data at time $t-1$. Actually, the control algorithms implemented for this prediction method are both deterministic MPC because the forecasting error variances would result in a value of σ_k^b too high to perform the stochastic MPC. For the "NO-PRED" prediction method, the results in Table 4 refers to the deterministic MPC described in Section 2.3.2, instead the results in Table 5 refers to the same deterministic MPC, but correcting the forecasting errors with the BESS; that is the deterministic MPC in Section 2.3.2 substituting (20)–(21) with (42)–(43).

The performance of the algorithms were tested on 30 days of simulation, from the midnight of July the 4th 2019 to the midnight of August the 3rd 2019. The reliability parameter β_k is not a constant value; in this application we considered a reliability that increases during the prediction horizon. Since it is that the smaller β_k, the higher θ_k, the uncertainties on far predictions are less weighted. The adopted values of β_k are:

- 0.025 for $k \in [0, 3]$;
- 0.05 for $k \in [4, 7]$;
- 0.075 for $k \in [8, 11]$;
- 0.1 for $k \in [12, 15]$;
- 0.15 for $k \in [16, 19]$;
- 0.25 for $k \in [20, PH-1]$.

A sensitivity study based on the length of the PH was carried out and the results of the control algorithms were evaluated on the REC income and, just for the stochastic MPC, on the algorithm failure rate, that is the times (as percentage of the all timestamps of simulation) the algorithm struggles to find the optimal condition. Table 4 shows the results obtained with the deterministic MPC algorithm and Table 5 those obtained with the stochastic MPC algorithm. We recall that the results in those tables only refers to the income of the REC, the actual

Table 3
REC study case parameters.

Parameter	Symbol	Value
Main Grid Connection Nominal Power	P^{g}_{max}	200 kW
BESS Nominal Charge Power	P^{ch}_{max}	120 kW
BESS Nominal Discharge Power	P^{dsc}_{min}	−120 kW
BESS Capacity	E	120 kW h
BESS Charge Efficiency	η^{ch}	95 %
BESS Discharge Efficiency	η^{dsc}	95 %
BESS maximum SoC	SoC^{max}	1
BESS minimum SoC	SoC^{min}	0
Maximum Number of complete Charge and Discharge Cycles	α	2
Aggregated Nominal Power Demand	P^{l}_{nom}	37.076 kW
Common Nominal Power Demand	P^{l}_{nom}	10.037 kW
PV Plant Nominal Power	P^{res}_{nom}	50 kW
MISE incentive	c^{m}	0.11 €/kWh
Restitution of Grid Charges	c^{r}	0.009 €/kWh

Table 4
Deterministic MPC results.

Prediction Method	REC Income [€]			% of ORACLE Income		
	Prediction Horizon			Prediction Horizon		
	12 h	18 h	24 h	12 h	18 h	24 h
LSTM1	2977	2967	2973	84.76	82.24	82.88
LSTM2	2976	2967	2961	84.71	82.26	82.55
biLSTM	3005	2974	2963	85.54	82.45	82.58
CNN–LSTM (96-2 × 1-32-48)	2913	2868	2856	82.93	79.51	79.62
CNN–LSTM (96-2 × 1-64-64)	2744	2798	2770	78.11	77.57	77.21
NO-PRED	2841	2959	2922	80.87	82.02	81.45
ORACLE	3513	3607	3588	100	100	100
TDNN-4–96	3178	3195	3153	90.47	88.59	87.89
TDNN-180–200	3219	3298	3272	91.64	91.44	91.20
TDNN-200–200	3238	3297	3266	92.18	91.41	91.05
TDNN-240–260	3245	3297	3265	92.36	91.40	91.02

economic gain of the REC members is given buy the REC income plus the savings on the electricity bill from the common load, i.e., €889 for the simulated period, paid at c^{e}. From both the tables it is possible to see how the algorithms fed with the predictions of the TDNNs performs better than the algorithms that receive in input the predictions obtained with the competitor neural networks. This happens for both the deterministic and stochastic MPC and for all the prediction horizon lengths investigated.

Moreover, the results obtained with the stochastic MPC are better than those obtained with the deterministic one, showing that maintaining the optimal profile of the power exchanged with the grid is the best solution from an economic point of view. The best achievable performance in terms of economic return is the one obtained with the stochastic MPC with a prediction horizon length $PH = 18$ h of €3600.75, as shown in Table 5. This does not directly reflect on the results obtained with the TDNNs. In fact, in these cases the best results are achieved with the TDNN-200-200 implementing a prediction horizon of length $PH = 12$ h; this particular length offers the smallest MAE in every predicted electrical energy feature for the TDNN-200-200 neural network, as shown in Table 1.

3.2.1. Selected prediction method — prediction horizon result

Among the couples Prediction Method — Prediction Horizon listed in Table 4 and in Table 5 the best one, in terms of income, is discussed in this section and the corresponding control variables profiles are shown for the week that goes from the midnight of July the 4th 2019 to July the 11th 2019. That is the case involving the TDNN-200-200 as prediction method and a prediction horizon length $PH = 12$ h. In particular, this case returns 96.73% of the maximum achievable income, i.e., the one obtained with the "ORACLE" prediction method, and allows a 18.72% increase in the income with respect to the "NO-PRED" prediction method.

The time-varying energy price c^{e}_{t}, which we assume the renewable energy is paid for, is shown in Fig. 4 and it refers to the actual energy clearing market price in Italy. Notice the energy prices considered in this application are referred to the values registered in the period going from the 4th of July 2021 to the 11th of July 2021.

The power profiles of PV generation, common power demand and residential buildings aggregated power demand are shown in Fig. 5.

Fig. 6 shows the optimal management strategy of the REC. From that, we can say that the REC manager tries to reduce the exported power P^{e} during the day by charging the BESS. By doing so P^{e}_{t} decreases, as it is stated by (17), to get closer to the value of P^{l}_{t}, optimizing the shared power P^{sh}_{t}, and the SoC rises ahead of the sunset, as shown in Fig. 7. During the night, the BESS can only be discharged, as it is stated by (16), thus, the BESS provides power. Often the discharge power of the BESS is not sufficient to satisfy the common load and the REC imports power from the grid. The negative values in Fig. 6 refer to imported power from the electric grid P^{i}_{t}.

Fig. 7 shows the power exchanged by the BESS, positive values refer to P^{ch}, while negative ones to P^{dsc}, and the SoC of the BESS, which is always limited between the time evolution of $\overline{SoC}$ (upper limit) and of $\underline{SoC}$ (lower limit). As a consequence of limiting the number of charge and discharge cycles evolution of the BESS seems to be quite monotonous in both charging and discharging phases, especially in the former one.

4. Conclusions

We presented a hybrid AI method for the optimal management of RECs. We proposed a method that provides an end-to-end approach: the predictions of a neural network concerning the aggregated load, the PV generation, and common services of a REC are passed as input to an optimization MPC algorithm to maximize the income. The method

Table 5
Stochastic MPC results.

Prediction Method	REC Income [€]			% of ORACLE Income			Failure Rate [%]		
	Prediction Horizon			Prediction Horizon			Prediction Horizon		
	12 h	18 h	24 h	12 h	18 h	24 h	12 h	18 h	24 h
LSTM1	3233	3169	3138	92.06	88.02	87.39	2.26	0.56	0.56
LSTM2	3252	3177	3118	92.58	88.23	86.85	0.28	0.45	0.45
biLSTM	3229	3197	3147	91.93	88.79	87.64	2.22	2.22	2.22
CNN–LSTM (96-2 × 1-32-48)	3180	3138	3082	90.55	87.15	85.84	0.56	0.03	0.10
CNN–LSTM (96-2 × 1-64-64)	3085	3116	3010	87.83	86.55	83.83	2.40	1.77	1.81
NO-PRED	2862	2991	2955	81.48	83.07	82.30	–	–	–
ORACLE	3512	3601	3591	100	100	100	–	–	–
TDNN-4–96	3347	3341	3206	95.29	92.80	89.28	–	–	0.31
TDNN-180–200	3378	3309	3268	96.18	91.91	91.01	–	–	2.43
TDNN-200–200	3398	3330	3295	96.73	92.47	91.76	–	–	0.45
TDNN-240–260	3395	3082	3268	96.66	85.60	91.02	–	0.17	0.38

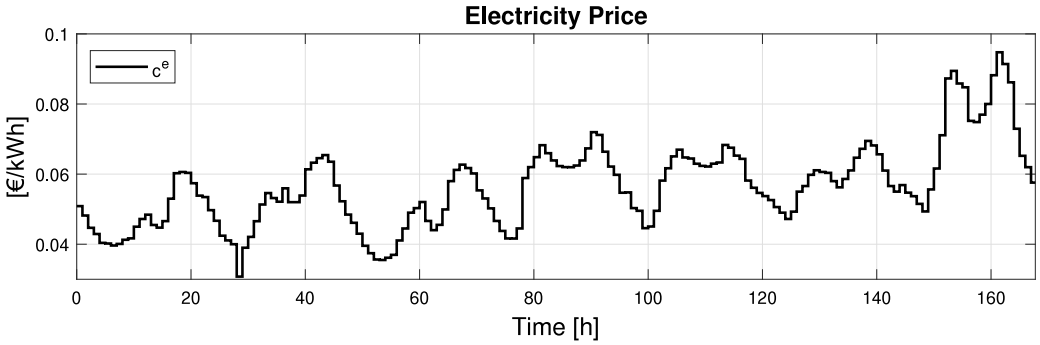

Fig. 4. Simulation data: energy price profile.

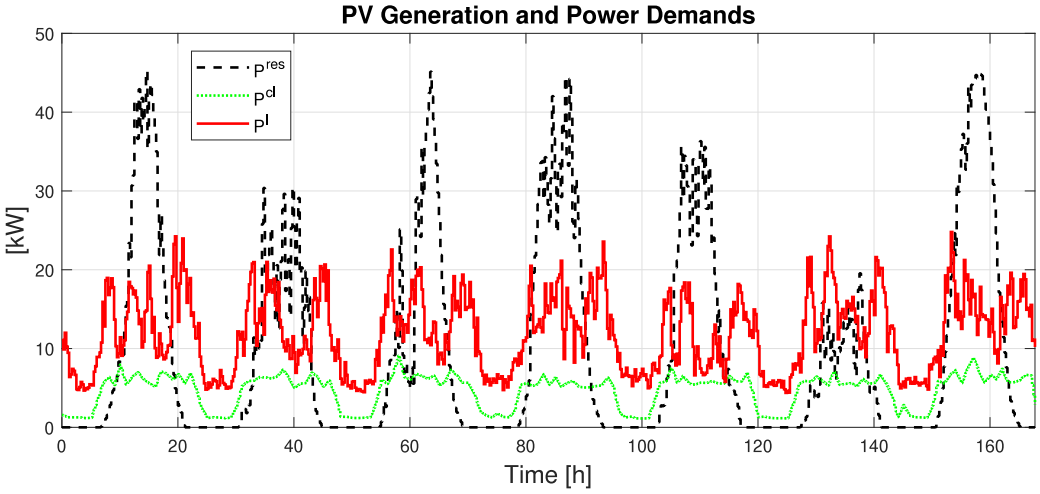

Fig. 5. Simulation data: PV generation, common power demand and building aggregated power demand profiles.

is validated on publicly-available data. The results of the proposed method are compared to those of several competitors. The proposed method generates the largest REC income. However, the present study has some limitations. The method is validated on data of a single REC, and thus, future studies must be directed towards further validation of the presented method on different public and private datasets. Also, it would be interesting to take into account more inputs such as the weather forecast for the prediction of future energy features, in order to achieve even better performance.

CRediT authorship contribution statement

Francesco Conte: Conceptualization, Methodology, Writing – review & editing, Supervision. **Federico D'Antoni:** Methodology, Software, Validation, Formal analysis, Investigation, Writing – original draft. **Gianluca Natrella:** Methodology, Software, Validation, Formal analysis, Investigation, Writing – original draft, Visualization. **Mario Merone:** Conceptualization, Methodology, Writing – review & editing, Supervision.

Declaration of competing interest

The authors declare that they have no known competing financial interests or personal relationships that could have appeared to influence the work reported in this paper.

Acknowledgment

All authors approved the version of the manuscript to be published.

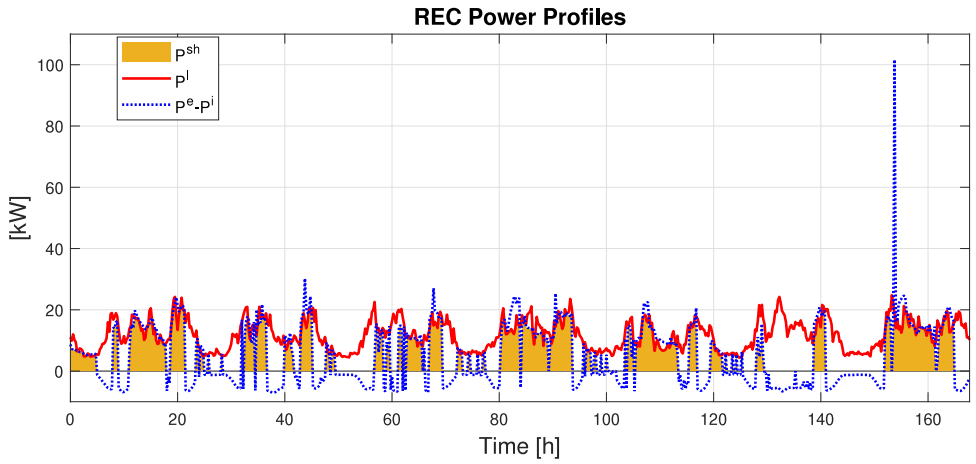

Fig. 6. REC power profiles.

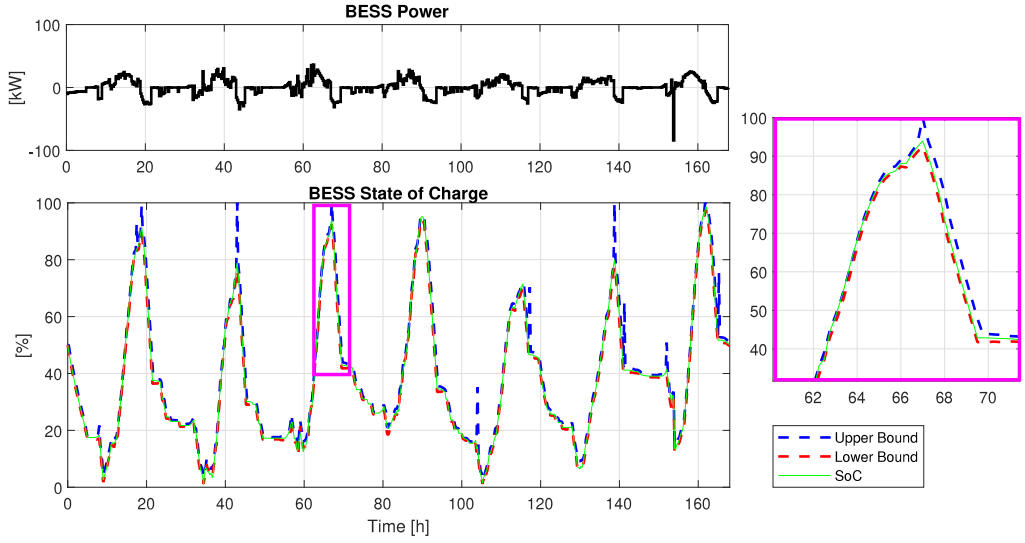

Fig. 7. Profiles of the power exchanged by the BESS, positive values refer to charge power, negative values refer to discharge power (top), and profile of the SoC of the BESS (bottom).

References

[1] Chang. UNC. The Paris agreement. 2015.

[2] Agency IE. World energy outlook 2017. 2017.

[3] European Commission, Directorate-General for Energy. In: Office P, editor. Clean energy for all Europeans. 2019.

[4] Grignani A, Gozzellino M, Sciullo A, Padovan D. Community cooperative: A new legal form for enhancing social capital for the development of renewable energy communities in Italy. Energies 2021;14(21). http://dx.doi.org/10.3390/en14217029.

[5] Italian Council of Ministers. DECRETO LEGISLATIVO 8 novembre 2021, n. 199 attuazione della direttiva (UE) 2018/2001 del parlamento europeo e del consiglio, dell'11 dicembre 2018, sulla promozione dell'uso dell'energia da fonti rinnovabili. 2021, [In Italian].

[6] Succetti F, Rosato A, Araneo R, Panella M. Deep neural networks for multivariate prediction of photovoltaic power time series. IEEE Access 2020;8:211490–505. http://dx.doi.org/10.1109/ACCESS.2020.3039733.

[7] Bruno S, Dellino G, La Scala M, Meloni C. A microforecasting module for energy consumption in smart grids. In: 2018 IEEE international conference on environment and electrical engineering and 2018 IEEE industrial and commercial power systems europe. IEEE; 2018, p. 1–6. http://dx.doi.org/10.1109/EEEIC.2018.8494345.

[8] Mariano-Hernández D, Hernández-Callejo L, Zorita-Lamadrid A, Duque-Pérez O, García FS. A review of strategies for building energy management system: Model predictive control, demand side management, optimization, and fault detect & diagnosis. J Build Eng 2021;33:101692. http://dx.doi.org/10.1016/j.jobe.2020.101692.

[9] Hazyuk I, Ghiaus C, Penhouet D. Optimal temperature control of intermittently heated buildings using model predictive control: Part II–control algorithm. Build Environ 2012;51:388–94. http://dx.doi.org/10.1016/j.buildenv.2011.11.008.

[10] Macarulla M, Casals M, Forcada N, Gangolells M. Implementation of predictive control in a commercial building energy management system using neural networks. Energy Build 2017;151:511–9. http://dx.doi.org/10.1016/j.enbuild.2017.06.027.

[11] Massa Gray F, Schmidt M. A hybrid approach to thermal building modelling using a combination of Gaussian processes and grey-box models. Energy Build 2018;165:56–63. http://dx.doi.org/10.1016/j.enbuild.2018.01.039.

[12] Hafiz F, de Queiroz AR, Fajri P, Husain I. Energy management and optimal storage sizing for a shared community: A multi-stage stochastic programming approach. Appl Energy 2019;236:42–54. http://dx.doi.org/10.1016/j.apenergy.2018.11.080.

[13] Parisio A, Glielmo L. Stochastic model predictive control for economic/environmental operation management of microgrids. In: 2013 european control conference. IEEE; 2013, p. 2014–9. http://dx.doi.org/10.23919/ECC.2013.6669807.

[14] Foroozandeh Z, Ramos S, Soares J, Lezama F, Vale Z, Gomes A, et al. A mixed binary linear programming model for optimal energy management of smart buildings. Energies 2020;13(7):1719. http://dx.doi.org/10.3390/en13071719.

[15] Koprinska I, Wu D, Wang Z. Convolutional neural networks for energy time series forecasting. In: 2018 international joint conference on neural networks. IEEE; 2018, p. 1–8. http://dx.doi.org/10.1109/IJCNN.2018.8489399.

[16] AEMO J. Australian energy market operator. 2016.

[17] Kingma DP, Ba J. Adam: A method for stochastic optimization. 2014, http://dx.doi.org/10.48550/arXiv.1412.6980, arXiv preprint arXiv:1412.6980.

[18] Barzola-Monteses J, Espinoza-Andaluz M, Mite-León M, Flores-Morán M. Energy consumption of a building by using long short-term memory network: a forecasting study. In: 2020 39th international conference of the chilean computer science society. IEEE; 2020, p. 1–6. http://dx.doi.org/10.1109/SCCC51225.2020.9281234.

[19] Kim T-Y, Cho S-B. Predicting residential energy consumption using CNN-LSTM neural networks. Energy 2019;182:72–81. http://dx.doi.org/10.1016/j.energy.2019.05.230.

[20] Hebrail G, Berard A. Individual household electric power consumption data set. uci machine learning repository. Irvine, CA: University of California, School of Information and Computer . . .; 2012.

[21] Olivella-Rosell P, Rullan F, Lloret-Gallego P, Prieto-Araujo E, Ferrer-San-José R, Barja-Martinez S, et al. Centralised and distributed optimization for aggregated flexibility services provision. IEEE Trans Smart Grid 2020;11(4):3257–69. http://dx.doi.org/10.1109/TSG.2019.2962269.

[22] Barone G, Brusco G, Menniti D, Pinnarelli A, Polizzi G, Sorrentino N, et al. How smart metering and smart charging may help a local energy community in collective self-consumption in presence of electric vehicles. Energies 2020;13(16):4163. http://dx.doi.org/10.3390/en13164163.

[23] Van Cutsem O, Dac DH, Boudou P, Kayal M. Cooperative energy management of a community of smart-buildings: A blockchain approach. Int J Electr Power Energy Syst 2020;117:105643. http://dx.doi.org/10.1016/j.ijepes.2019.105643.

[24] Wen L, Zhou K, Yang S, Lu X. Optimal load dispatch of community microgrid with deep learning based solar power and load forecasting. Energy 2019;171:1053–65. http://dx.doi.org/10.1016/j.energy.2019.01.075.

[25] Inc. PS. Dataport, URL https://dataport.pecanstreet.org/.

[26] Arkhangelski J, Mahamadou A-T, Lefebvre G. Data forecasting for optimized urban microgrid energy management. In: 2019 IEEE international conference on environment and electrical engineering and 2019 IEEE industrial and commercial power systems europe. IEEE; 2019, p. 1–6. http://dx.doi.org/10.1109/EEEIC.2019.8783853.

[27] England IN. Community Energy data.

[28] Hong T, Pinson P, Wang Y, Weron R, Yang D, Zareipour H. Energy forecasting: A review and outlook. IEEE Open Access J Power Energy 2020;7:376–88. http://dx.doi.org/10.1109/OAJPE.2020.3029979.

[29] Hobbs BF, Jitprapaikulsarn S, Konda S, Chankong V, Loparo KA, Maratukulam DJ. Analysis of the value for unit commitment of improved load forecasts. IEEE Trans Power Syst 1999;14(4):1342–8. http://dx.doi.org/10.1109/59.801894.

[30] Ramos S, Soares J, Foroozandeh Z, Tavares I, Vale Z. Energy consumption and PV generation data of 15 prosumers (15 minute resolution). Zenodo 2021. http://dx.doi.org/10.5281/zenodo.5106455.

[31] Peddinti V, Povey D, Khudanpur S. A time delay neural network architecture for efficient modeling of long temporal contexts. In: Sixteenth annual conference of the international speech communication association. 2015, p. 3214–8. http://dx.doi.org/10.21437/Interspeech.2015-647.

[32] Møller MF. A scaled conjugate gradient algorithm for fast supervised learning. Neural Netw 1993;6(4):525–33. http://dx.doi.org/10.1016/S0893-6080(05)80056-5.

[33] European Commission. Revised renewable energy directive (2018/2001/EU). 2018.

[34] European Commission. Directive on common rules for the internal electricity market ((EU) 2019/944). 2019.

[35] Wang JQ, Du Y, Wang J. LSTM based long-term energy consumption prediction with periodicity. Energy 2020;197:117197. http://dx.doi.org/10.1016/j.energy.2020.117197.